Magnetic Resonance Imaging 108 (2024) 104–110

Contents lists available at ScienceDirect

Magnetic Resonance Imaging

journal homepage: www.elsevier.com/locate/mri

Constrained spherical deconvolution on diffusion-weighted images of dolphin brains

Tommaso Gerussi [a,*], Jean-Marie Graïc [a], Bruno Cozzi [a], Lara Schlaffke [b,c], Onur Güntürkün [d,e], Mehdi Behroozi [d,*]

[a] Department of Comparative Biomedicine and Food Science (BCA), University of Padua, Legnaro, Italy
[b] Department of Neurology, BG-University Hospital Bergmannsheil, Ruhr-University Bochum, Bürkle-de-la-Camp-Platz 1, 44789 Bochum, Germany
[c] Heimer Institute for Muscle Research, BG-University Hospital Bergmannsheil, Bochum, Germany
[d] Department of Biopsychology, Institute of Cognitive Neuroscience, Faculty of Psychology, Ruhr-University Bochum, 44801 Bochum, Germany
[e] Research Center One Health Ruhr, Research Alliance Ruhr, Ruhr-University Bochum, Bochum, Germany

ARTICLE INFO

Keywords:
DWI
CSD
Ex-vivo
Tractography
Dolphin
Large brain

ABSTRACT

Invasive neuronal tract-tracing is not permitted in very large or endangered animals. This is especially the case in marine mammals like dolphins. Diffusion-weighted imaging of fiber tracts could be an alternative if feasible even in brains that have been fixed in formalin for a long time. This currently is a problem, especially for detecting crossing fibers. We applied a state-of-the-art algorithm of Diffusion-weighted imaging called Constrained Spherical Deconvolution on diffusion data of three fixed brains of bottlenose dolphins using clinical human MRI parameters and were able to identify complex fiber patterns within a voxel. Our findings indicate that in order to maintain the structural integrity of the tissue, short-term post-mortem fixation is necessary. Furthermore, preprocessing steps are essential to remove the classical Diffusion-weighted imaging artifacts from images: however, the algorithm is still able to resolve fiber tracking in regions with various signal intensities. The described imaging technique reveals complex fiber patterns in cetacean brains that have been preserved in formalin for extended periods of time and thus opens a new window into our understanding of cetacean neuroanatomy.

1. Introduction

Cetaceans are aquatic mammals characterized by elaborate social interactions, complex behaviors, and outstanding cognitive abilities [9,12]. However, practical and ethical reasons make *in vivo* studies on the neuroanatomical basis of their cognitive capabilities impossible. However, recent advances in magnetic resonance imaging (MRI) have provided a set of non-invasive tools to even investigate postmortem brains. Diffusion-weighted imaging (DWI) is a non-invasive method to measure the diffusion process of the water molecules in biological tissues which can be used to map white matter tractography [7,13]. Diffusion Tensor Imaging (DTI) is a mathematical model applied to DWI data, based on the ability to detect and quantify the anisotropic diffusion of water molecules in white matter tissue. DTI is represented with an ellipsoid which gives the microstructural characteristics and the orientation of each voxel [2,3]. Fiber tracking or "diffusion tractography" is the result of combining the orientation of every voxel. However, DTI's main drawback is that it is insensitive to complex fiber architectures, specifically because it is unable to identify crossing fibers which limits its application to study complex neural pathways [1,11,19]. During the last decade, multiple mathematical algorithms have been developed to overcome this limitation and yield excellent results in living human brains that reasonably approximate clinical parameters. The constrained spherical deconvolution (CSD, [19]) is a performant algorithm that reconstructs white matter tracts by estimating the distribution of fiber orientation (fFOD), based on an estimate of the response function of a single fiber that matches the common signal profile obtained from white matter [1,11].

To the best of our knowledge, until now, there are only three studies that investigated tractography in dolphin brains, using the DTI method [4,14,22]. While DTI has already proved efficacy in *ex-vivo* tissues, CSD use has been limited to *in-vivo* brains. However, a recent study demonstrated the feasibility of using CSD in fixed dolphin brains in the investigation of prefrontal cortex connections [8]. In the current study, we report the application, feasibility, and results of CSD applied to post-mortem fixed brains of bottlenose dolphins (*Tursiops truncatus*, Montagu

* Corresponding authors.
E-mail addresses: tommaso.gerussi@studenti.unipd.it (T. Gerussi), Mehdi.Behroozi@ruhr-uni-bochum.de (M. Behroozi).

https://doi.org/10.1016/j.mri.2024.02.002
Received 7 March 2023; Received in revised form 2 February 2024; Accepted 3 February 2024
Available online 8 February 2024

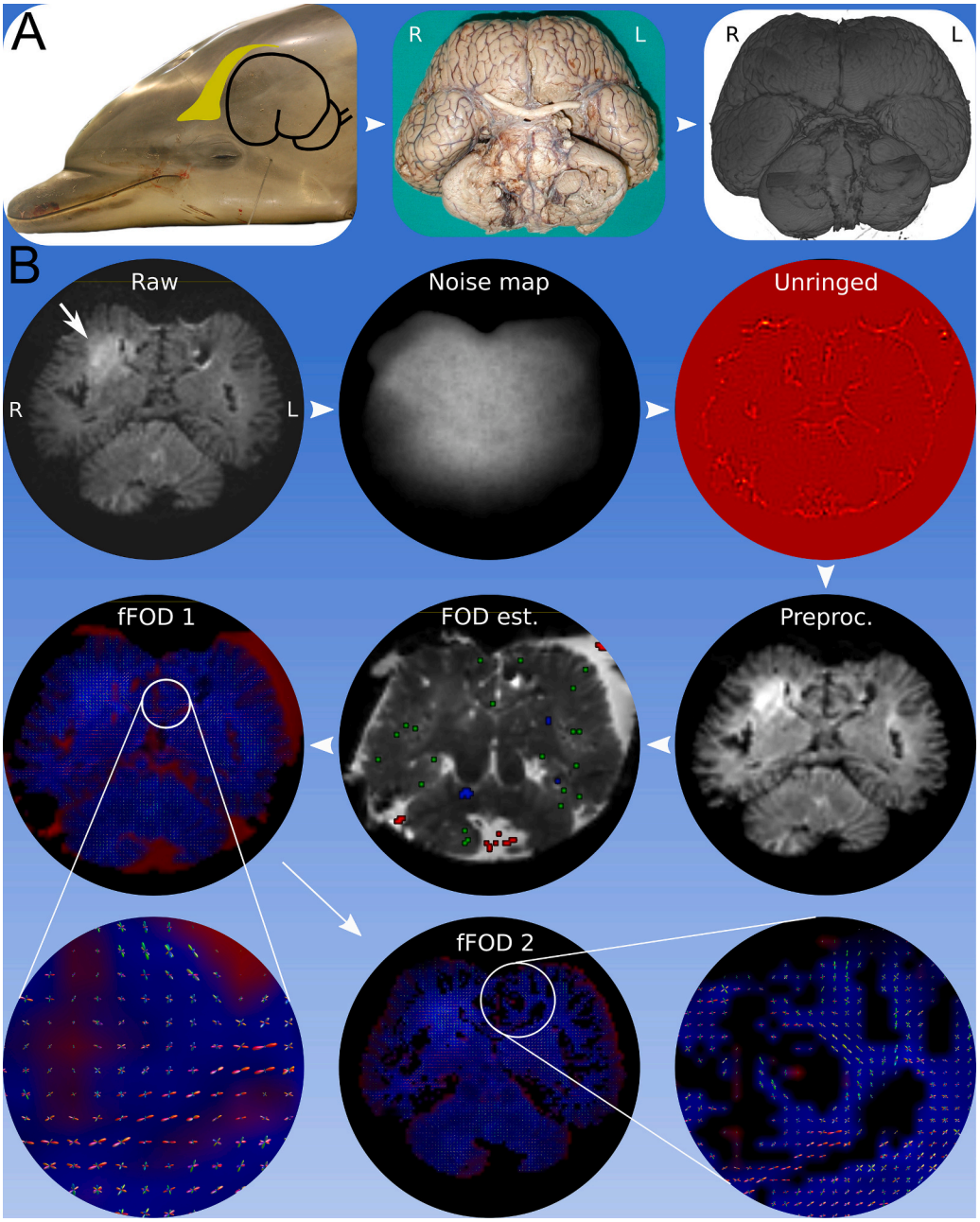

Fig. 1. Schematic overview of the various pre-processing steps of the CSD analysis. (A) Location of the brain in the head (left); fixed brain (central) and 3D model of the scanned brain (right) of a bottlenose dolphin. (B) DWI processing steps. Raw, raw data directly from the MRI scanner, the arrow indicates a bright area; Noise map, map of the noise which has been corrected; Unringed, overlap of the denoised and unringed images; Preproc., preprocessed data; FOD est., response function estimation with dhollander algorithm and subsequent division between three different tissues: WM (blue), GM (green), liquid/CSF (red); fFOD 1, first FOD calculation without a mask and consequent imprecise division between tissues (magnification in the circle); fFOD 2, second FOD calculation with a mask and better estimation of WM (magnification in the circle). (For interpretation of the references to colour in this figure legend, the reader is referred to the web version of this article.)

1821). We consider the quality and reliability of the results and discuss the difficulties when applying this technique to fixed cetacean brains. It is worth noting that two of these brains have been preserved for more than two decades. This long period of fixation presents unique challenges and considerations, which we discuss and address in our analysis.

2. Materials and methods

2.1. Specimens

For this research, we used formalin-fixed brains of three bottlenose dolphins (*Tursiops truncatus*, Montagu 1821). The brains belonged to two adult females (age: fixation time > 20 years) and one adult male specimen (age: fixation time > 5 years).

These animals were transported to the Department of Comparative Biomedicine and Food Science (BCA) of the University of Padova for post-mortem diagnosis and the samples collected were stored in the *Mediterranean Marine Mammal Tissue Bank* (MMMTB, http://www.marinemammals.eu). The MMMTB is a CITES-recognized (IT020) research center, collaborating with and sponsored by the University of Padova and the Italian Ministry of the Environment, as well as other Italian organizations working with marine mammals.

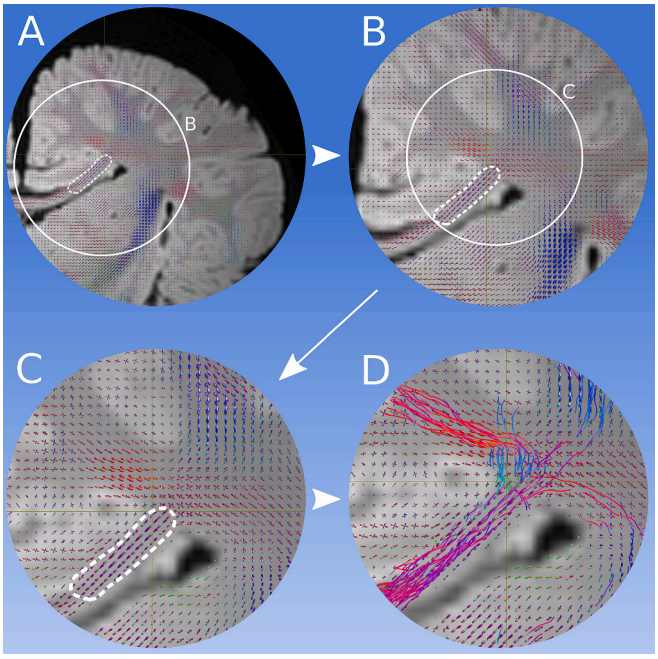

Fig. 2. Visualization of a ROI involving the corpus callosum (dotted area) in a coronal view. A → C: increasing of magnification to verify the correct orientation of the fFOD. D: After the application of tractography, note how the fibers are straight and grouped in the main bundle but then split to go to the rest of the cortex.

The brains were extracted from the skull 5 to 10 h after death and directly fixed by immersion in neutral buffered paraformaldehyde (PFA 4% changed on a regular basis). The animals died of non-neurological reasons and the brains showed no macroscopic evidence of damage, suffering or illness. Fig. 1 A illustrates the position of the brain, its ventral view and a comparable 3D MRI. One of the brains was divided in two and the cerebellum was removed for other research purposes. The brain size ranged from 152 to 190 mm (latero-lateral), 110 to 125 mm (dorso-ventral) and 123 to 154 mm (rostro-caudal).

2.2. Data acquisition

Before MRI scans, brains were sealed in plastic bags with a small amount of PFA 4% to avoid direct air contact. The scans were acquired using a 32-channel head coil on a 3 T human MRI system (Achieva 3 T X, Philips). T_2-weighted structural images were acquired through a 3D fast acquisition with Fast Field Echo Imaging (FFE) in the axial plane using the following parameters: FFE factor = 105; field of view (FOV) = 150.0 × 200.0× 150.0 cm^3; repetition time/echo time (TR/TE) = 8.2/3.8 ms; matrix size = 152 × 201; the number of slices = 150; voxel size = 1.0 × 1.0 × 1.0 mm^3. The total acquisition time per brain was 6 min and 26 s. A single-shot Echo Planar Imaging (EPI) sequence was used to obtain DW images in the axial plane with the following parameters: EPI factor = 41; FOV = 224 × 168 × 150 cm^3; TR/TE = 23.200/88 ms; matrix size = 112 × 82; the number of slices = 75; voxel size = 2.0 × 2.0 × 2.0 mm^3; diffusion-weighting along 60 directions with b = 3500 s/mm^2. One non-diffusion-weighted image (b_0) was acquired for each specimen. The total acquisition time per brain was 24 min and 21 s. To overcome the geometry distortion of the EPI sequence, 2 additional DW images (b =

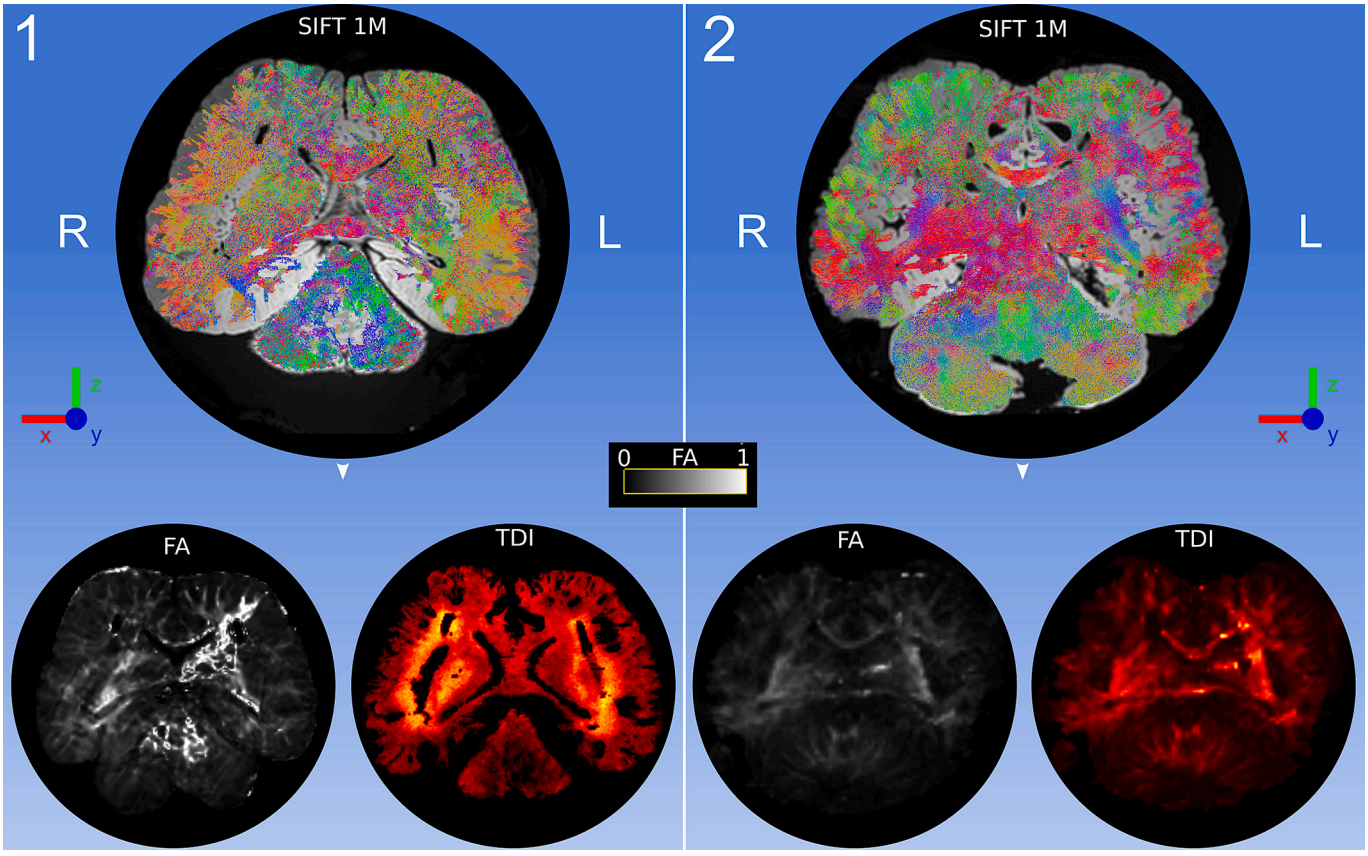

Fig. 3. Global tractogram of the male (1) and female (2) bottlenose dolphins. Top: SIFT 1 M, whole brain tracking after SIFT application. Bottom: FA, FA map which intensity varied between 0 and 1; TDI, track density imaging. The colours reflected the direction along the MRI scanner; x, latero-lateral; y, dorso-ventral and z, cranio-caudal. Colour codes were as follows: red: latero-lateral; blue: dorso-ventral; and green: cranio-caudal. (For interpretation of the references to colour in this figure legend, the reader is referred to the web version of this article.)

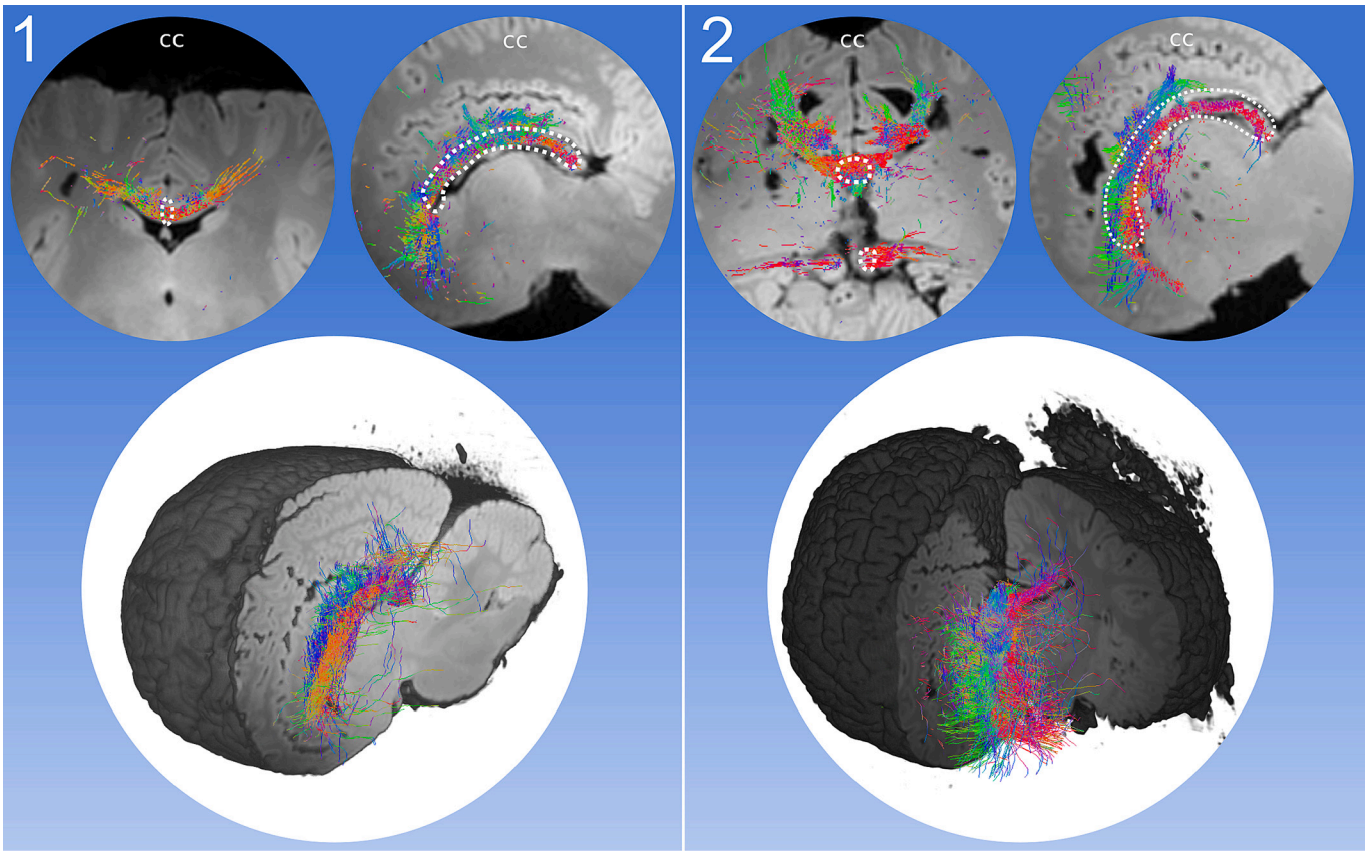

Fig. 4. Regional tractogram of the corpus callosum (cc) of the male (1) and female (2) bottlenose dolphins from SIFT 1 M. Tracts are represented in axial (top-left), sagittal (top-right) and 3D oblique (bottom) views. The colours reflected the direction along the MRI scanner; x, latero-lateral; y, dorso-ventral and z, cranio-caudal. Colour codes were as follows: red: latero-lateral; blue: dorso-ventral; and green: cranio-caudal. Dotted circles indicate the ROIs were drawn. (For interpretation of the references to colour in this figure legend, the reader is referred to the web version of this article.)

3500 s/mm^2) and 2 non-DW images were acquired in the opposite phase encoding direction.

2.3. Data processing

DWI data were processed for voxel-based analysis using FSL (version 6.0.5.1, https://fsl.fmrib.ox.ac.uk/fsl/fslwiki, [10,16,21]) and MRtirx3 (https://www.mrtrix.org/; [20]) software. The DWI data processing steps for each individual were as follows: (i) converting Dicom files to ".mif" format, (ii) denoising using Marchenko-Pastur principal component analysis, (iii) Gibbs ringing removal, (iv) motion and distortion correction (including Eddy current distortions and susceptibility-induced EPI distortions) using the opposite phase encoding direction images, and (v) bias field correction to eliminate low-frequency intensity inhomogeneities across the image. Subsequently, the dhollander algorithm was applied to estimate different response functions for the white matter (WM, anisotropic), cerebrospinal fluid, and grey matter (CSF and GM, both isotropic; [6]). fFOD was then calculated by first taking the estimation of dhollander algorithm into consideration to then use a mask in which most of the neocortical grey matter was manually removed for better biological plausibility (*i.e.* absence of tracts in the CSF and GM).

2.4. Tractography

The whole brain tractogram was generated using the iFOD2 algorithm (Second-order Integration over Fiber Orientation Distributions) - a probabilistic algorithm that takes the fFOD file as an input. This method is capable to precisely track crossing fibers and fibers in highly curved areas. The following default MRtrix parameters were used: FOD amplitude threshold = 0.1, step size = 0.2 mm, and angle threshold = 60°. The first streamline count was set to ten million but since one of the drawbacks of the CSD is the over-representation of long tracts to the detriment of short tracts, a *spherical-deconvolution informed filtering of tracks* (SIFT) algorithm was applied by a factor of 10, yielding a total of one million tracts. The fractional anisotropy (FA) was calculated. This index reflects the main fiber organization within each voxel based on the degree of freedom of water molecules in the axons. Since it varies from 0 (completely isotropic = free movement in three dimensions) to 1 (completely anisotropic = restricted movement in one dimension), its values were then superimposed on the obtained tracts file to verify that areas with high anisotropy, such as the corpus callosum, had a higher value of areas rich in crossing fibers such as the grey matter. This parameter allowed us to verify the general quality of our results including the preservation of geometry and orientation (Figs. 2,3; Suppl. Mat. 1, 2). In addition, we ran a region of interest (ROI) analyses by placing seeds in some brain regions such as the corpus callosum (cc, Fig. 4), the optic tract (OT, Fig. 5), the pons (Fig. 6), the internal capsule (Suppl. Mat. 1) and the spinal cord (Suppl. Mat. 2). A few hyperintense regions were visible in the diffusion raw data of two specimens, possibly due to some technical issues during brain fixation. However even these regions were included in the tractography to minimize the processing steps and keep them similar to *in-vivo* scans. Controls were performed by comparing areas containing these hyperintense areas with the contralateral intact equivalents, to check for any abnormality between the two sides (Suppl. Mat. 3).

For further details in the "Data processing" and "Tractography" sections concerning the methodology and the references, see the complete and exhaustive step-by-step description in the B.A.T.M.A.N.

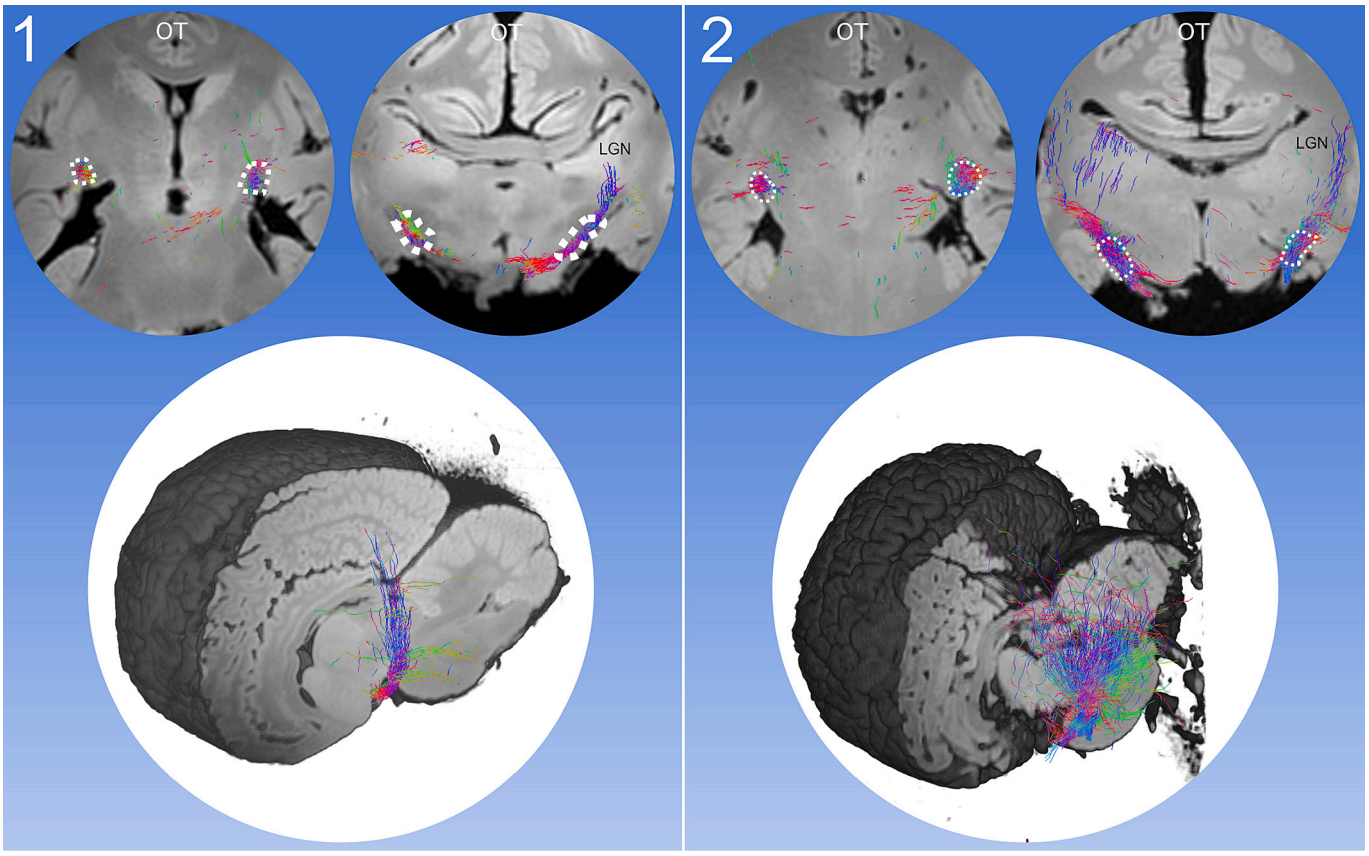

Fig. 5. Regional tractogram of the optic tract (OT) of the male (1) and female (2) bottlenose dolphins from SIFT 1 M. Tracts are represented in axial (top-left), coronal (top-right) and 3D oblique (bottom) views. The colours reflected the direction along the MRI scanner; x, latero-lateral; y, dorso-ventral and z, cranio-caudal. Colour codes were as follows: red: latero-lateral; blue: dorso-ventral; and green: cranio-caudal. Dotted circles indicate the ROIs were drawn. LGN, lateral geniculate nucleus. (For interpretation of the references to colour in this figure legend, the reader is referred to the web version of this article.)

tutorial (https://osf.io/fkyht/).

3. Results

The combination of the MRI clinical protocols and the improvement of the mathematical algorithms for DWI image sequence analysis allowed us to scan and perform CSD analysis in formalin-fixed bottlenose dolphin brains. Figs. 3–6 shows the results of the steps previously described and the selected ROIs analyses for two specimens (for the third specimen, see Supplementary Materials). All pre-processing steps improved the quality of the images. Some bright spots remained (Fig. 1, arrow), but the algorithm was able to overcome these defects which probably resulted from local areas that were not perfectly fixed (Suppl. Mat. 3).

Global tracking after applying the SIFT algorithm allowed to correct the biases caused by the CSD and showed a reduction in fiber density (Fig. 3, first row) that, combined with the FA map, resembled the biological plausibility of the direction of the fibers (Fig. 3, second row). Overall, all the ROI analyses were qualitatively satisfying, thus allowing us to isolate more regions from the same tractogram. Unfortunately, we only had two separated hemispheres in the third brain, resulting in a misalignment during scanning (Suppl. Mat. 1). In all three brains, the cc showed fibers with a latero-lateral and cranial trend (Fig. 4, Suppl. Mat. 1). Fibers of the OT ran in a dense patch until they reached the lateral geniculate nucleus (Fig. 5, Suppl. Mat. 1). In the two intact brains, fibers seeding the ventral part of the pons followed the middle cerebellar peduncle reaching the cerebellum (Fig. 6) and fibers isolated from the spinal cord split into a streamline rostral-oriented band that followed the corticospinal tract and a bundle that followed the inferior cerebellar peduncle into the cerebellum (Suppl. Mat. 2). Finally, seeding the thalamus, the fibers reached the neocortex following the internal capsule (Supplementary material, Fig. 1).

4. Discussion

The few published electrophysiological experiments and tracing studies performed on bottlenose dolphins or smaller harbor porpoises (*Phocoena phocoena*) revealed four primary brain areas: auditory, visual, motor, and somatosensory cortices, and their relation with the thalamic nuclei [15,17]. Invasive studies have ever since been abandoned and all subsequent studies were based on *ex-vivo* brains.

In the meantime, the development of new instruments improved the value of imaging techniques in human diagnostics and had a positive influence on the progress of comparative neuroscience research. So far, CSD was applied mostly to the *in-vivo* human brain and is rarely used to explore other species. In our study, we evaluate the feasibility of this technique in postmortem dolphin brains, considering its methodological limits, and its application to large formalin-fixed brains [18].

Overall, our pre-processing steps successfully compensated potential problems of fixed brains like hyperintense areas and generated data for CSD analysis. CSD results showed that the nervous tissues were generally very well preserved even after prolonged formalin fixation. This was qualitatively demonstrated in two ways: first, the directions of the fibers were correct and homogeneous throughout the whole brain (see Fig. 2–6); second, the FA map superimposed to the tracts indicated their most plausible direction. This is, *e.g.* visible in the corpus callosum where the fibers were all directed towards the same direction.

The hyperintense regions, already discussed above, could influence

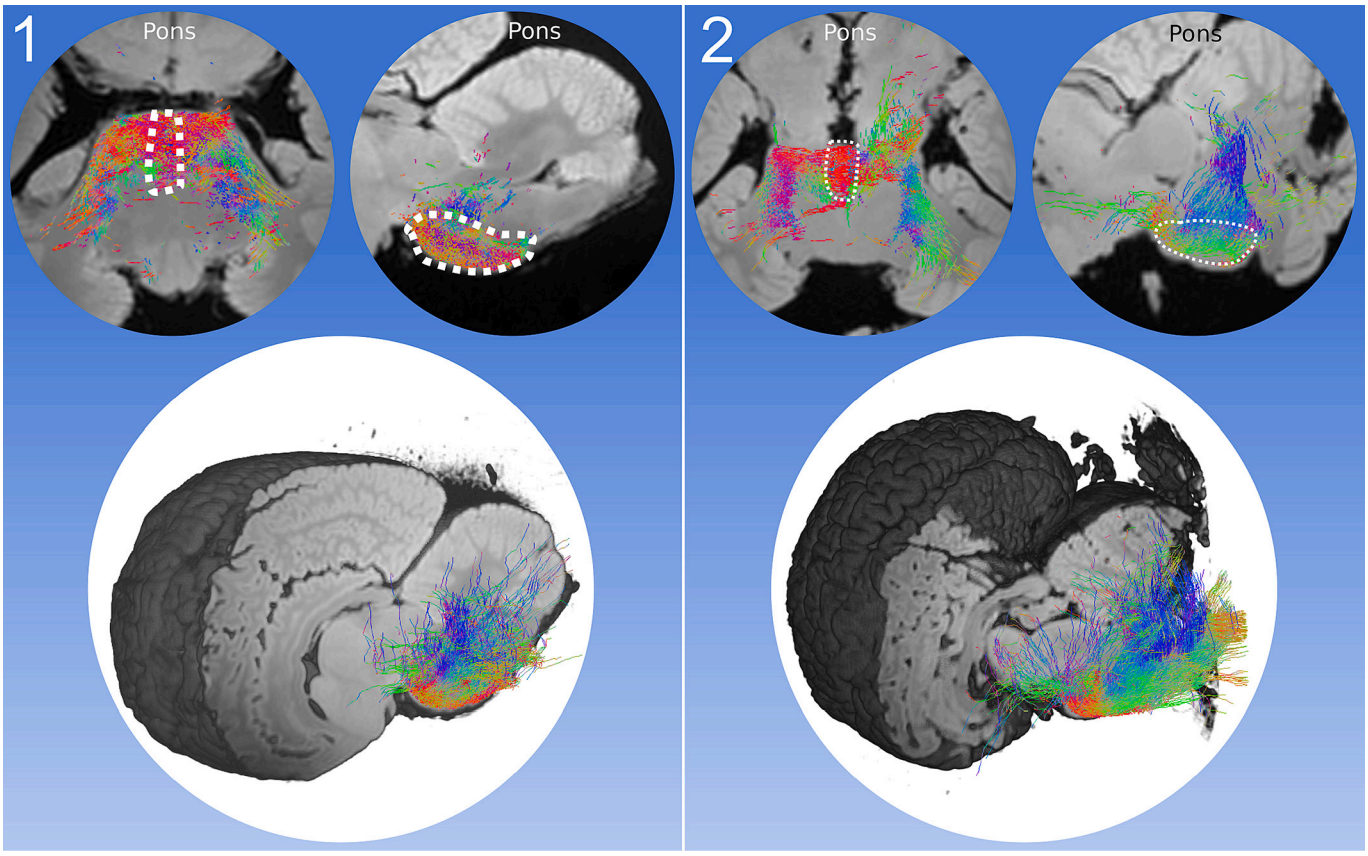

Fig. 6. Regional tractogram of the pons of the male (1) and female (2) bottlenose dolphins from SIFT 1 M. Tracts are represented in axial (top-left), sagittal (top-right) and 3D oblique (bottom) views. The colours reflected the direction along the MRI scanner; x, latero-lateral; y, dorso-ventral and z, cranio-caudal. Colour codes were as follows: red: latero-lateral; blue: dorso-ventral; and green: cranio-caudal. Dotted circles indicate the ROIs were drawn. (For interpretation of the references to colour in this figure legend, the reader is referred to the web version of this article.)

the FOD estimation, fFOD calculation, and thus streamline densities in that area. However, our employed algorithm was able to select only the most important fiber populations, omitting aberrant extras.

Optimal or satisfactory fixation of the brain of large wild species is a challenge. Postmortem interval, bodily conditions, and environmental factors can compromise a timely and thorough fixation. The *algor mortis* that occurs in human cadavers and brings within 24 h the internal temperature to an equilibrium with the external environment is not present in dolphins and larger cetaceans, because of the body fat that maintains a high internal temperature for longer periods and worsens autolytic processes. The anatomy of the arterial supply to the dolphin brain, with the absence of patent internal carotid arteries in the adult and the presence of the retia mirabilia [5], makes fixation by perfusion very complicated and often unsuccessful. Fixation by immersion remains an acceptable method, especially when the brain is stored in abundant and cold aldehydes that delay autolysis and allow penetration to the inner parts of the organ. Our results show that formalin-fixed brains may yield important data on the functional organization of the brain of species otherwise difficult to study. Taken all together, *ex-vivo* DWI may represent an important research tool for comparative neuroscientists. It provides whole-brain access to investigate connectivity in fixed brains, even in those fixed for years. The ability to investigate structural connectivity in post-mortem brains opens up a new research window to study the central nervous system of rare and highly protected species.

CRediT authorship contribution statement

Tommaso Gerussi: Writing – original draft, Visualization, Methodology, Conceptualization. **Jean-Marie Graïc:** Visualization. **Bruno Cozzi:** Writing – review & editing, Visualization. **Lara Schlaffke:** Writing – review & editing, Data curation. **Onur Güntürkün:** Writing – original draft, Conceptualization. **Mehdi Behroozi:** Writing – original draft, Visualization, Supervision, Methodology, Formal analysis, Data curation.

Declaration of competing interest

The authors declare that they have no known competing financial interests or personal relationships that could have appeared to influence the work reported in this paper.

Acknowledgments

Supported by a grant from the German Research Council to OG (Gu 227/16-1); and from the University of Padova D.O.R. Bruno Cozzi.

Appendix A. Supplementary data

Supplementary data to this article can be found online at https://doi.org/10.1016/j.mri.2024.02.002.

References

[1] Arrigo A, Calamuneri A, Mormina E. Diffusion MRI of human brain: key points and innovations. Global J Med Res 2016;16(D1):11–5. Retrieved from https://medicalresearchjournal.org/index.php/GJMR/article/view/1112.
[2] Basser PJ, Le Bihan D. Fiber orientation mapping in an anisotropic medium with NMR diffusion spectroscopy. In: Proceedings of the 11th annual meeting of the SMRM; 1992. p. 1221.

[3] Basser PJ, Pajevic S, Pierpaoli C, et al. In vivo fiber tractography using DT-MRI data. Magn Reson Med 2000;44:625–32. https://doi.org/10.1002/1522-2594(200010)44:4<625::aid-mrm17>3.0.co;2-o.
[4] Berns GS, Cook PF, Foxley S, Jbabdi S, Miller KL, Marino L. Diffusion tensor imaging of dolphin brains reveals direct auditory pathway to temporal lobe. Proc Royal Soc B: Biol Sci 2015;282(1811):20151203. https://doi.org/10.1098/rspb.2015.1203.
[5] Cozzi B, Huggenberger S, Oelschläger HA. Anatomy of dolphins: Insights into body structure and function. Elsevier Academic Press; 2017 [eBook ISBN: 9780124076556].
[6] Dhollander T, Raffelt D, Connelly A. Unsupervised 3-tissue response function estimation from single-shell or multi-shell diffusion MR data without a co-registered T1 image. 2016 [ISMRM Workshop on Breaking the Barriers of Diffusion MRI].
[7] Dubois J, Hertz-Pannier L, Dehaene-Lambertz G, et al. Assessment of the early organization and maturation of infants' cerebral white matter fiber bundles: a feasibility study using quantitative diffusion tensor imaging and tractography. NeuroImage 2006;30:1121–32. https://doi.org/10.1016/j.neuroimage.2005.11.022.
[8] Gerussi T, Graïc J-M, Peruffo A, Behroozi M, Schlaffke L, Huggenberger S, et al. The prefrontal cortex of the bottlenose dolphin (Tursiops truncatus Montagu, 1821): a tractography study and comparison with the human. Brain Struct Funct 2023;228(8):1963–76. https://doi.org/10.1007/s00429-023-02699-8.
[9] Güntürkün O. Is dolphin cognition special? Brain Behav Evol 2014;83(3):177–80. https://doi.org/10.1159/000357551.
[10] Jenkinson M, Beckmann CF, Behrens TE, Woolrich MW, Smith SM. FSL Neuroimage 2012;62(2):782–90. https://doi.org/10.1016/j.neuroimage.2011.09.015.
[11] Jeurissen B, Descoteaux M, Mori S, Leemans A. Diffusion MRI fiber tractography of the brain. NMR Biomed 2019;32(4):e3785. https://doi.org/10.1002/nbm.3785.
[12] Loth A, Güntürkün O, von Fersen L, Janik VM. Through the looking glass: how do marked dolphins use mirrors and what does it mean? Anim Cogn 2022;25(5):1151–60. https://doi.org/10.1007/s10071-022-01680-y.
[13] Moseley ME, Cohen Y, Kucharczyk J, et al. Diffusion-weighted MR imaging of anisotropic water diffusion in cat central nervous system. Radiology 1990;176:439–45. https://doi.org/10.1148/radiology.176.2.2367658.
[14] Orekhova K, Selmanovic E, De Gasperi R, et al. Multimodal assessment of bottlenose dolphin auditory nuclei using 7-tesla MRI, immunohistochemistry and stereology. Vet Sci 2022;9(12):692. https://doi.org/10.3390/vetsci9120692.
[15] Revishchin AV, Garey LJ. The thalamic projection to the sensory neocortex of the porpoise, Phocoena phocoena. J Anat 1990;169:85 [PMID: 2384340].
[16] Smith SM, Jenkinson M, Woolrich MW, Beckmann CF, Behrens TEJ, Johansen-Berg H, et al. Advances in functional and structural MR image analysis and implementation as FSL. Neuroimage 2004;23(1):208–19. https://doi.org/10.1016/j.neuroimage.2004.07.051.
[17] Supin AY, Popov VV, Mass AM. The sensory Phyiology of aquatic mammals. Boston, MA: Springer US; 2001. https://doi.org/10.1007/978-1-4615-1647-7.
[18] Tax CM, Jeurissen B, Vos SB, Viergever MA, Leemans A. Recursive calibration of the fiber response function for spherical deconvolution of diffusion MRI data. Neuroimage 2014;86:67–80. https://doi.org/10.1016/j.neuroimage.2013.07.067.
[19] Tournier JD, Calamante F, Connelly A. Robust determination of the fibre orientation distribution in diffusion MRI: non-negativity constrained super-resolved spherical deconvolution. NeuroImage 2007;35:1459–72. https://doi.org/10.1016/j.neuroimage.2007.02.016.
[20] Tournier JD, Smith R, Raffelt D, Tabbara R, Dhollander T, Pietsch M, et al. MRtrix3: a fast, flexible and open software framework for medical image processing and visualisation. Neuroimage 2019;202:116137. https://doi.org/10.1016/j.neuroimage.2019.116137.
[21] Woolrich MW, Jbabdi S, Patenaude B, Chappell M, Makni S, Behrens T, et al. Bayesian analysis of neuroimaging data in FSL. NeuroImage 2009;45(1):173–86. https://doi.org/10.1016/j.neuroimage.2008.10.055.
[22] Wright AK, Theilmann RJ, Ridgway SH, Scadeng M. Diffusion tractography reveals pervasive asymmetry of cerebral white matter tracts in the bottlenose dolphin (Tursiops truncatus). Brain Struct Funct 2018;223(4):1697–711. https://doi.org/10.1007/s00429-017-1525-9.